Minimal diffusion formulation of Markov chain ensembles and its application to ion channel clusters

Marifi Güler*
Department of Computer Engineering, Eastern Mediterranean University, Famagusta, via Mersin-10, Turkey
(Received 19 November 2014; published 12 June 2015)

We study ensembles of continuous-time Markov chains evolving independently under a common transition rate matrix in some finite state space. A diffusion approximation, composed of two specifically coupled Ornstein-Uhlenbeck processes in stochastic differential equation representation, is formulated to deduce how the number of chains in a given particular state evolves in time. This particular form of the formulation builds upon a theoretical argument adduced here. The formulation is minimal in the sense that it is always a two-dimensional stochastic process regardless of the state space size or the transition matrix density, and that it requires no matrix square root operations. A set of criteria, put forward here as to be necessarily captured by any consistent approximation scheme, is used together with the master equation to determine uniquely the parameter values and noise variances in the formulation. The model is applied to the gating dynamics in ion channel clusters.

DOI: 10.1103/PhysRevE.91.062116 PACS number(s): 05.40.Ca, 02.50.Ga, 87.16.dj, 87.16.Vy

I. INTRODUCTION

Motions governed by Markov chains are the most commonly applied class of stochastic processes in science and engineering [1,2]. In this paper, we consider not just one Markov chain but an ensemble of chains. The chains in the ensemble are assumed to be evolving independently in the same finite state space with some continuous-time Markov transition rules common to all the chains. The primary objective of this study was to deduce the temporal evolution of the number of chains in a prescribed *relevant state*. Although the analysis of the temporal evolution of one Markov chain is comparatively easy, the mathematics becomes quite complicated for the collective behavior of a population of chains. In this context, Kurtz [3] has approximated density-dependent Markov processes, for large system size, down to a diffusion model represented by a system of stochastic differential equations (for a detailed account, see Ref. [4]). The Kurtz approach was later rediscovered by Fox and Lu [5] in the study of ion channel clusters. Density-dependent processes have appeared in a variety of biological and physical contexts, including chemical kinetics, ecological models, epidemics, metapopulations, telecommunications, and computational neuroscience (e.g., see Refs. [5,6]).

The use of the diffusion approximation is, however, deterred by the inherent requirement of calculation of a matrix square root at each time step in it. In addition, the number of noise terms required there increases with the state space size. Recently, approaches that circumvent the matrix square root calculations were introduced [7,8], but at the expense that the number of noise terms employed does not only increase with the state space size, but also with the transition rate matrix density. This extra increase in the number of noise terms continues to be the case even when one is interested in the dynamics specific to the relevant state only. The approaches of Refs. [7,8] yield the same resulting formulation (see the Appendix in Ref. [9]). These approaches derive from the fact that different but equivalent Itô stochastic differential equation models of random dynamical systems can be constructed [10].

Our diffusion approximation formulated here, on the other hand, is minimal in the sense that it accommodates only two stochastic variables (correspondingly two noise terms) irrespective of the state space size or the transition matrix density and is not hindered by the matrix square root operations; therefore, it provides a simple analytic formulation and a fast computation algorithm for the problem. This is made possible by treating the effect of the state density fluctuations, other than that of the relevant state, collectively instead of using the density fluctuations of the individual states explicitly. The approximation is formulated as a two-dimensional stochastic process comprised of two specifically coupled Ornstein-Uhlenbeck processes in stochastic differential equation representation. This form of the formulation stems from a theoretical argument that we present later in this paper. The parameter values and noise variances in the formulation are determined uniquely by means of a set of criteria put forward here as to be necessarily captured by any consistent approximation scheme. This requires the knowledge of the expectation value of the number of chains in a given state, which is easily computed from the master equation deterministically.

We apply our model to the gating by ion channel clusters to illustrate its accuracy in reproducing the statistical properties of the exact microscopic Markov simulations. These channels facilitate excitability of cells [11]. The gating of ion channels is typically modeled by means of a continuous-time discrete state Markovian kinetic scheme, in which, a channel can be open (the relevant state) or else it is found in one of the multiple closed states.

II. AVERAGE STATE DENSITIES

Consider N ergodic (irreducible) continuous-time Markov chains evolving independently under a common transition rate matrix in the finite space of states $\{0,1,\ldots,L\}$. Let $\theta_l\,(l = 0,1,\ldots,L)$ be the number of chains in state l at a particular time, and refer to the synonym $\psi_l := \theta_l/N$ as the density of state l. Symbolize the fluctuation in the state density ψ_l by ϕ_l, that is,

$$\psi_l := \langle\psi_l\rangle + \phi_l, \quad (l = 0,1,\ldots,L), \tag{1}$$

*marifi.guler@gmail.com

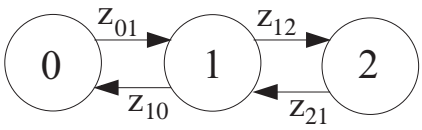

FIG. 1. Example state transition diagram used in demonstrating the implementation of the master equation. z's are the transition rates.

where $\langle\cdots\rangle$ denotes the expectation value. Note that the average state density $\langle\psi_l\rangle$ corresponds to the probability of finding a chain in state l. $\langle\psi_l\rangle$ are, in general, time-dependent quantities. By definition, it reads that

$$\sum_{l=0}^{L}\langle\psi_l\rangle = 1. \tag{2}$$

The evolution of the expectation values $\langle\psi_l\rangle\,(l = 0,1,\ldots,L)$ can be computed from the L coupled linear deterministic differential equations governed by the master equation. A fundamental property of the master equation in Markov processes is that, as $t \to \infty$, all solutions tend to a stationary solution if the state set contains strictly a finite number of discrete states and the transition rates are constant in time. There exists only one stationary solution if the transition rate matrix is not decomposable. Therefore, with constant transition rates, $\langle\psi_l\rangle\,(l = 0,1,\ldots,L)$ reaches to the unique steady state in the long-time limit. We assume the transition rates to be constant in our analysis in the next section, but later allow them to be slowly varying.

For demonstration, consider the example state transition diagram given in Fig. 1. In this particular case, the master equation reads

$$\begin{aligned}
\frac{d\langle\psi_0\rangle}{dt} &= -z_{01}\langle\psi_0\rangle + z_{10}\langle\psi_1\rangle,\\
\frac{d\langle\psi_1\rangle}{dt} &= z_{01}\langle\psi_0\rangle - (z_{10}+z_{12})\langle\psi_1\rangle + z_{21}\langle\psi_2\rangle,\\
\frac{d\langle\psi_2\rangle}{dt} &= z_{12}\langle\psi_1\rangle - z_{21}\langle\psi_2\rangle,
\end{aligned} \tag{3}$$

where z's are the transition rates and Eq. (2) becomes

$$\langle\psi_0\rangle + \langle\psi_1\rangle + \langle\psi_2\rangle = 1. \tag{4}$$

For time-dependent transition rates, the average state densities can be solved iteratively from Eq. (3). For constant transition rates, the steady state

$$\frac{d\langle\psi_0\rangle}{dt} = \frac{d\langle\psi_1\rangle}{dt} = \frac{d\langle\psi_2\rangle}{dt} = 0 \tag{5}$$

prevails in the long-time limit. Then, after noting that only two of the equations in the set given by Eq. (3) are linearly independent, Eqs. (3)–(5) uniquely solve $\langle\psi_0\rangle$, $\langle\psi_1\rangle$, and $\langle\psi_2\rangle$.

III. THE RELEVANT STATE DENSITY FLUCTUATIONS: SPECIAL CASE

In formulating the dynamics of the fluctuation ϕ_r, where the subscript r stands for the relevant state, let us start with the special case that the relevant state is directly connected only to one state—say, to state s—in the transition diagram

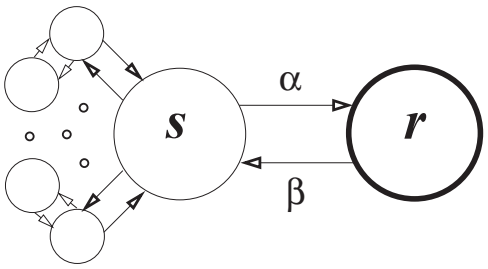

FIG. 2. Sketch of the relevant state when it makes a direct connection with one state only.

(see Fig. 2). Assume that the transition rates α and β, shown in Fig. 2, are positive constants. Recall that our formalism presumes an equilibrium framework, and therefore, the equations below derived for the evolution of state density fluctuations hold after the relaxation of the system.

A. Theory and the derivation

This section gives the underlying theory, and correspondingly the derivation, of our minimal diffusion formulation. The reader impatient to use or implement the governing equations, however, might prefer to jump directly to the next section.

Note that, by definition, we have

$$\sum_{l=0}^{L}\psi_l = 1. \tag{6}$$

Then it follows from Eqs. (1) and (2) that

$$\sum_{l=0}^{L}\phi_l = 0 \tag{7}$$

and

$$\langle\phi_l\rangle = 0, \quad (l = 0,1,\ldots,L). \tag{8}$$

In addition, we need the second moments of the fluctuations. It follows from the dispersion relation of the binomial distribution that

$$\left\langle\phi_l^2\right\rangle = \frac{\langle\psi_l\rangle(1-\langle\psi_l\rangle)}{N}, \quad (l = 0,1,\ldots,L). \tag{9}$$

One can also derive, for any two different states l and m, that

$$\langle\phi_l\phi_m\rangle = -\frac{\langle\psi_l\rangle\langle\psi_m\rangle}{N}, \quad l \neq m. \tag{10}$$

Regarding states l and m as a single combined state and applying Eq. (9) yields

$$\langle(\phi_l+\phi_m)^2\rangle = \frac{(\langle\psi_l\rangle+\langle\psi_m\rangle)(1-\langle\psi_l\rangle-\langle\psi_m\rangle)}{N},$$

which, in turn, results in Eq. (10).

In the designated special case, the relevant state density fluctuation ϕ_r changes in time under the control of the stochastic differential equation [5,7]

$$\dot{\phi}_r = -\beta\phi_r + \alpha\phi_s + \xi, \tag{11}$$

where ξ is mean zero Gaussian white noise with the mean square

$$\langle \xi(t)\xi(t')\rangle = \frac{\alpha\langle\psi_s\rangle + \beta\langle\psi_r\rangle}{N}\delta(t-t'). \tag{12}$$

The variance of the noise ξ used here, however, slightly differs from Refs. [5,7] by the presence of expectation values on the right side of Eq. (12). The fluctuation ϕ_s in Eq. (11) cannot be determined by itself without solving all the state density fluctuations ϕ_l ($l = 0,1,\ldots,L$) simultaneously at each time step when the current approaches [3,7,8] are used. Further difficulties are faced with the use of these approaches. In the approach of Kurtz [3], the number of noise terms required increases with the state space size and some matrix square root calculations have to be performed at each time step. Although the approaches of Refs. [7,8] avoid the matrix square root operations, it is at the expense that the number of noise terms then does not only increase with the state space size but also with the density of the transition rate matrix. Our diffusion approximation developed here, on the other hand, does not suffer from any of these difficulties as it does not require individual use of the state density fluctuations other than ϕ_r and ϕ_s; instead, the collective effect of these other density fluctuations is implicitly incorporated into the formulation.

Concerning the state density fluctuation ϕ_s, it is obvious that

(i) ϕ_s must necessarily counterbalance the variation caused by ξ in ϕ_r due to Eq. (25a);

(ii) $\langle\phi_s^2\rangle$ must agree with Eq. (9);

(iii) $\langle\phi_s\phi_r\rangle$ must agree with Eq. (10).

These criteria, however, do not suffice to uniquely identify ϕ_s. We therefore introduce a method that facilitates unique identification of ϕ_s, when used together with the above criteria. The method is as below.

Define $\phi_{\mathbf{H}} := (\phi_l | l \neq s)$ and assume that the system identified by the array $\phi_{\mathbf{H}} \times \phi_s = (\phi_l | l = 0,1,\ldots,L)$ has had enough time to reach equilibrium. Note that the space of values that $\phi_{\mathbf{H}}$ can attain is dependent on ϕ_s due to Eq. (7) and that the space changes in time as ϕ_s varies. Let $T(\phi_{\mathbf{H}}^{(2)} \times \phi_s^{(2)}, t_2 \mid \phi_{\mathbf{H}}^{(1)} \times \phi_s^{(1)}, t_1)$ denote the transition probabilities that governs the temporal evolution of the system $\phi_{\mathbf{H}} \times \phi_s$ at equilibrium. Now suppose that we perform an exact microscopic Markov simulation of the system in a thought experiment and obtain a vast number of stochastic evolution paths of $\phi_{\mathbf{H}} \times \phi_s$ and then measure a new type of transition probabilities $\overline{T}(\phi_s^{(2)}, t_2 | \phi_s^{(1)}, t_1)$ over the paths collectively. Here $\overline{T}(\phi_s^{(2)}, t_2 \mid \phi_s^{(1)}, t_1)$ is not decided by a single measurement, but rather assumed to be obtained from the average of collective measurements, subject to $\phi_s(t_1) = \phi_s^{(1)}$ and $\phi_s(t_2) = \phi_s^{(2)}$, over the $\phi_{\mathbf{H}} \times \phi_s$ paths generated. Then consider some function $f(\phi_s(t), \phi_s(t'))$. Let $\langle f\rangle_T$ and $\langle f\rangle_{\overline{T}}$ denote f's expectation values as computed using the transition probabilities T and $\overline{T}$, respectively. It accordingly applies that $\langle f\rangle_T = \langle f\rangle_{\overline{T}}$. Thus, in computing the expectation values of functions of ϕ_s, we can use $\overline{T}$ instead of T.

The process ϕ_s characterized by the transition probability $\overline{T}$, at equilibrium, is Markovian and stationary. It can also be regarded as a Gaussian process, even though this is only approximately true. Therefore, the process is an Ornstein-Uhlenbeck process. This is due to Doob's theorem, which states that if a process is simultaneously Markovian, stationary, and Gaussian, then it is either an Ornstein-Uhlenbeck process or a completely random process. An Ornstein-Uhlenbeck process is represented by a stochastic differential equation in the form of Langevin equation. Thus, we employ an equation for the evolution of ϕ_s,

$$\dot{\phi}_s = -\gamma\phi_s - \xi + \eta, \tag{13}$$

where η is a mean zero Gaussian white noise independent of ξ (i.e., $\langle\eta\xi\rangle = 0$). The term ξ is the same noise as in Eqs. (11) and (12). The $-\xi$ term in Eq. (13) was included for counterbalancing ξ's effect on ϕ_r. The parameter γ and the variance of η are determined below.

The differential equations (11) and (13) have the solutions

$$\phi_r(t) = e^{-\beta t}\left\{\phi_r(0) + \int_0^t e^{\beta t'}\left[\alpha\phi_s(t') + \xi(t')\right]dt'\right\} \tag{14}$$

and

$$\phi_s(t) = e^{-\gamma t}\left\{\phi_s(0) - \int_0^t e^{\gamma t'}[\xi(t') - \eta(t')]dt'\right\}, \tag{15}$$

respectively. From these equations, we calculate $\langle\phi_s^2\rangle$ and $\langle\phi_s\phi_r\rangle$ at equilibrium, i.e., in the long-time limit. It follows from Eq. (15), using $\langle\eta\xi\rangle = 0$, that

$$\langle\phi_s(t)^2\rangle = e^{-2\gamma t}\int_0^t\int_0^t e^{\gamma(t_1+t_2)}[\langle\xi(t_1)\xi(t_2)\rangle + \langle\eta(t_1)\eta(t_2)\rangle]dt_1dt_2, \tag{16}$$

which, in turn, gives

$$\langle\phi_s^2\rangle = \frac{\langle\xi^2\rangle + \langle\eta^2\rangle}{2\gamma} \tag{17}$$

in the limit $t \to \infty$. Note that, on the course of derivation, we have taken the expectation values out of the integral, as their values are constants at equilibrium; which we utilize also in the below derivation. It reads from Eqs. (14) and (15) that

$$\langle\phi_s(t)\phi_r(t)\rangle = e^{-\beta t}\int_0^t e^{\beta t'}[\alpha\langle\phi_s(t)\phi_s(t')\rangle + \langle\phi_s(t)\xi(t')\rangle]dt'. \tag{18}$$

Utilizing

$$\langle\phi_s(t)\xi(t')\rangle = -\langle\xi^2\rangle e^{-\gamma(t-t')}, \quad t \geqslant t',$$

and employing the autocorrelation function of the Langevin motion [12]

$$\langle\phi_s(t')\phi_s(t)\rangle = \langle\phi_s^2\rangle e^{-\gamma(t-t')}, \quad t \geqslant t',$$

yields that

$$\langle\phi_s\phi_r\rangle = \frac{\alpha\langle\phi_s^2\rangle - \langle\xi^2\rangle}{\gamma+\beta}. \tag{19}$$

Solving Eqs. (17) and (19) for γ and $\langle\eta^2\rangle$ simultaneously and substituting $\langle\phi_s^2\rangle$ and $\langle\phi_s\phi_r\rangle$ with their corresponding values given by Eqs. (9) and (10), respectively, derives that

$$\gamma = \frac{\alpha\langle\psi_s\rangle^2 + \beta\langle\psi_r\rangle(1 - \langle\psi_s\rangle)}{\langle\psi_s\rangle\langle\psi_r\rangle} \tag{20}$$

and

$$\langle \eta(t)\eta(t')\rangle = \frac{\alpha\langle\psi_s\rangle C_\alpha + \beta\langle\psi_r\rangle C_\beta}{N\langle\psi_r\rangle}\delta(t-t'), \tag{21}$$

where C_α and C_β stand for

$$\begin{aligned} C_\alpha &:= 2\langle\psi_s\rangle(1-\langle\psi_s\rangle) - \langle\psi_r\rangle, \\ C_\beta &:= 2(1-\langle\psi_s\rangle)^2 - \langle\psi_r\rangle. \end{aligned} \tag{22}$$

Thus, the above criteria for $\langle\phi_s^2\rangle$ and $\langle\phi_s\phi_r\rangle$ uniquely identify the friction coefficient γ and the noise η.

Although γ given by Eq. (20) is unconditionally non-negative, it is not the case for $\langle\eta^2\rangle$ given by Eq. (21). If $\langle\psi_r\rangle$ is within a certain proximity of its steady state value, then $\langle\eta^2\rangle$ is guaranteed to be non-negative, which is just fine as our analysis presumes an equilibrium framework. To see this, consider the master equation for $\langle\psi_r\rangle$:

$$\frac{d\langle\psi_r\rangle}{dt} = -\beta\langle\psi_r\rangle + \alpha\langle\psi_s\rangle, \tag{23}$$

which reads at the steady state as

$$\beta\langle\psi_r\rangle = \alpha\langle\psi_s\rangle. \tag{24}$$

Inserting Eq. (24) into Eq. (21) yields

$$\langle\eta^2\rangle = \frac{2\beta}{N}[1-\langle\psi_s\rangle - \langle\psi_r\rangle],$$

which is by Eq. (2) always non-negative.

Since the nearly Gaussian process ϕ_s, characterized by the transition probability $\overline{T}$, was taken to be exactly Gaussian in developing our formulation, the error of our formulation is expected to be larger than the error of diffusion approximation by Kurtz. However, we anticipate still the same order of error in both models. Kurtz has given a bound on the order of error of his diffusion approximation as $O(\ln N/N)$ [3].

B. Governing model equations and implementation issues

The evolution of ϕ_r, in our model, is thus given by the coupled stochastic differential equations

$$\dot{\phi}_r = -\beta\phi_r + \alpha\phi_s + \xi, \tag{25a}$$

$$\dot{\phi}_s = -\gamma\phi_s - \xi + \eta, \tag{25b}$$

where the parameter γ is as given by Eq. (20). The terms ξ and η are independent mean zero Gaussian white noises with the mean squares given by Eqs. (12) and (21), respectively. Then, solving ϕ_r from the formulation here and using $\langle\psi_r\rangle$ as obtained from the master equation, we conclude the evolution of ψ_r by means of $\psi_r = \langle\psi_r\rangle + \phi_r$.

Although we have assumed the transition rates to be constant in our analysis in the preceding section, the governing equations can be safely used also with slowly varying transition rates. Then, the average state densities $\langle\psi_l\rangle\,(l=0,1,\ldots,L)$ need to be obtained iteratively from the master equation. Correspondingly, note that despite that the noise variance $\langle\eta^2\rangle$, defined by Eq. (21), is guaranteed to be non-negative when $\langle\psi_r\rangle$ is within the proximity of its steady state value, it may be negative during the initial transient period in an iterative numerical implementation. In such case, η may be set to zero or the absolute value $|\langle\eta^2\rangle|$ may be used for the variance.

In applying Euler's method for the numerical solution of Eq. (25b), the step size Δt should satisfy, for the stability reasons, that $\Delta t\,\gamma < 1$. However, γ can attain large values, which dictates the usage of a very small Δt, or else ϕ_s can be set directly to zero for γ values that violate the inequality $\Delta t\,\gamma < 1$.

The above formulation is essentially the same also in the case when the relevant state makes direct connection with an arbitrary number of states: It then only requires a modification of α, β, and $\langle\psi_s\rangle$, as to be given in Sec. IV.

As seen, our formulation does not require matrix square root operations and contains only two stochastic variables—ϕ_r and ϕ_s—for any state space size or transition matrix density. Clearly, it is very much simpler than the formulations of Kurtz [3] or Orio and Soudry [7] and offers a faster computation algorithm. This point is discussed further in Sec. V, together with making reference also to the model by Güler [13] that was developed in the context of ion channels.

IV. GENERALIZATION

We next consider the case that the relevant state directly connects to two states, say, to states j and k. Assume that the transition rates from the state r to states j and k are denoted by β_j and β_k, respectively, and the rates from j to r and from k to r are denoted by α_j and α_k, respectively. Then ϕ_r evolves in accordance with

$$\dot{\phi}_r = -(\beta_j+\beta_k)\phi_r + \alpha_j\phi_j + \alpha_k\phi_k + \xi. \tag{26}$$

Instead of dealing with the states j and k explicitly, here we substitute them by a single effective state s with the objective of being able to use the above formulation, developed for the case of one-state direct connection, also in this case.

Define new parameters α and β and set

$$\beta = \beta_j + \beta_k. \tag{27}$$

Then making substitution $\alpha_j\phi_j + \alpha_k\phi_k \to \alpha\phi_s$ converts Eq. (26) to Eq. (25a). For the effective state s to be treated as a single state, the following must be satisfied:

(i) $\alpha\langle\psi_s\rangle = \alpha_j\langle\psi_j\rangle + \alpha_k\langle\psi_k\rangle$;
(ii) $\langle\psi_s\rangle$ abides by Eq. (23);
(iii) $\langle\phi_s^2\rangle$ agrees with Eq. (9);
(iv) $\langle\phi_s\phi_r\rangle$ agrees with Eq. (10);
(v) $\langle\psi_s\rangle + \langle\psi_r\rangle \leqslant 1$.

The necessary and sufficient condition for these requirements to hold is that the parameter α and the probability $\langle\psi_s\rangle$ are set as

$$\alpha = A + \frac{B}{A} \tag{28}$$

and

$$\langle\psi_s\rangle = \frac{A^2}{A^2+B}, \tag{29}$$

with

$$\begin{aligned} A &:= \alpha_j\langle\psi_j\rangle + \alpha_k\langle\psi_k\rangle, \\ B &:= \alpha_j^2\langle\psi_j\rangle(1-\langle\psi_j\rangle) - 2\alpha_j\alpha_k\langle\psi_j\rangle\langle\psi_k\rangle \\ &\quad + \alpha_k^2\langle\psi_k\rangle(1-\langle\psi_k\rangle). \end{aligned} \tag{30}$$

The proof is as follows. The first requirement directly reads from Eqs. (28) and (29). In this case, the master equation implies that

$$\frac{d\langle\psi_r\rangle}{dt} = -\beta\langle\psi_r\rangle + \alpha_j\langle\psi_j\rangle + \alpha_k\langle\psi_k\rangle,$$

which, under the first requirement, reads in the same form as Eq. (23). Comparison of Eq. (26) with Eq. (25a) shows that

$$\phi_s = \frac{\alpha_j\phi_j + \alpha_k\phi_k}{\alpha},$$

which gives

$$\langle\phi_s\phi_r\rangle = \frac{\alpha_j\langle\phi_j\phi_r\rangle + \alpha_k\langle\phi_k\phi_r\rangle}{\alpha}$$

and

$$\langle\phi_s^2\rangle = \frac{\alpha_j^2\langle\phi_j^2\rangle + 2\alpha_j\alpha_k\langle\phi_j\phi_k\rangle + \alpha_k^2\langle\phi_k^2\rangle}{\alpha^2}.$$

In turn, using Eqs. (9) and (10) yields

$$\langle\phi_s\phi_r\rangle = -\langle\psi_r\rangle\frac{A}{\alpha N} \quad \text{and} \quad \langle\phi_s^2\rangle = \frac{B}{\alpha^2 N},$$

where A and B are as given by Eq. (30). It then follows that $\langle\phi_s^2\rangle$ and $\langle\phi_s\phi_r\rangle$ agree with Eqs. (9) and (10), respectively, provided that α and $\langle\psi_s\rangle$ are set to be as given by Eqs. (28) and (29), respectively. Suppose that the inequality $\langle\psi_s\rangle + \langle\psi_r\rangle \leqslant 1$ holds. Then, multiplying both sides of it by α and using Eqs. (28) and (29) implies that $A \leqslant \alpha(1 - \langle\psi_r\rangle)$, which, in turn, gives

$$A^2 \leqslant (A^2 + B)(1 - \langle\psi_r\rangle). \tag{31}$$

On the other hand, we have that $\langle\psi_j\rangle + \langle\psi_k\rangle \leqslant 1 - \langle\psi_r\rangle$. Then, if the inequality

$$A^2 \leqslant (A^2 + B)(\langle\psi_j\rangle + \langle\psi_k\rangle) \tag{32}$$

holds, so does (31). After substituting A and B, Eq. (32) gives $0 \leqslant (\alpha_j - \alpha_k)^2$. Thus, the inequality $\langle\psi_s\rangle + \langle\psi_r\rangle \leqslant 1$ is indeed satisfied.

To sum up, the governing equations are valid also in the case of two-state direct connection once the settings (27)–(30) are done. Moreover, to extend the formulation to a case where the relevant state makes direct connection with arbitrary number of states, one only needs to modify β defined by Eq. (27) and the parameters A and B in Eq. (30). Assume that the relevant state directly connects to the set of states D. Then, the modifications to be made are

$$\beta = \sum_{i\in D}\beta_i, \quad A = \sum_{i\in D}\alpha_i\langle\psi_i\rangle,$$

and

$$B = N\left\langle\left(\sum_{i\in D}\alpha_i\phi_i\right)^2\right\rangle. \tag{33}$$

The resulting second moments in Eq. (33) can be easily computed from Eqs. (9) and (10).

At this point, we mention a study [14] which partly motivated our present work. The study argues that the computing time of the exact microscopic Markov simulations can be shortened considerably, without significant loss in accuracy, by regarding fluctuations only in those states directly connected to the relevant state in every chain. That conjecture, in a sense, is similar to the one we used in this work, but our utilization of the conjecture is different. First, contrary to our formulation, the simulation method in Ref. [14] violates the criterion that $\langle\phi_s\phi_r\rangle$ agrees with Eq. (10). Second, instead of ignoring the fluctuations in those states that are not directly connected to the relevant state, our diffusion approximation implicitly reflects the collective effect of these fluctuations into the formulation. Third, the simulation method needs an increasing number of noise terms with the increase in the number of states directly connected to the relevant state, whereas there is no such increase in our formulation. Of course, unlike the diffusion models but like any microscopic Markov simulation algorithm, the computational complexity of that simulation method still increases with the number of chains.

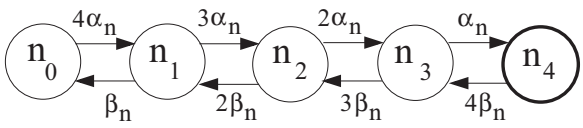

FIG. 3. State transition diagram of a potassium channel.

V. APPLICATION TO ION CHANNEL CLUSTERS

The excitability of cells is facilitated by voltage-gated ion channels. Each type of ion channel is selective to conduct a particular ion species, and that the transmembrane conductance of potassium and sodium is controlled by these channels [11]. The number of open channels fluctuates in a seemingly random manner [15], which results in a fluctuation in the conductivity of the membrane and, in turn, a fluctuation in the transmembrane voltage. When the number of ion channels (i.e., the cell's membrane area) is very large, the voltage fluctuations become negligible, and, therefore, the transmembrane voltage dynamics is then described by the celebrated Hodgkin-Huxley (HH) equations [16]. For smaller membrane patches, however, the effects of the channel fluctuations are potentially profound. The stochastic behavior of ion channels is generally characterized by continuous-time, discrete-state Markov jump processes [17]. State transition diagrams of potassium and sodium channels are given in Figs. 3 and 4, respectively. Note that there exist four n gates in a potassium channel and three m gates and one h gate in a sodium channel.

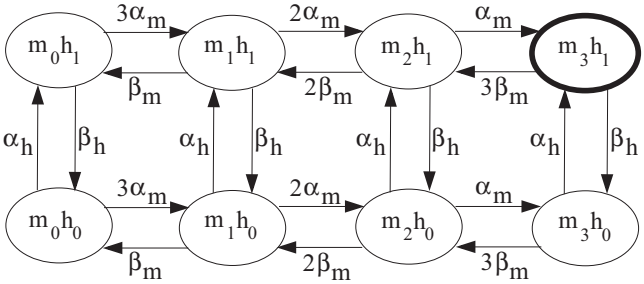

FIG. 4. State transition diagram of a sodium channel.

A channel is open when all of its gates are open; otherwise, it is closed. There is no mutual interaction among the channels.

Microscopic Markov simulation of a population of channels can be pursued by the simple stochastic method that keeps track of each Markov process for the state of each gate simultaneously. Although faster microscopic methods, based on the well-known Gillespie algorithm, that need to keep track only of the total populations of channels in each possible state are available [18], the computational complexity necessarily increases with the number of channels. As a result, there has been high motivation for developing an alternative formulation that approximates the microscopic dynamics efficiently without computational cost increase with population size. In a pioneering work in this line of research, Fox and Lu [5] developed a diffusion approximation to the discrete gate dynamics in which the vector containing the fractions of possible channel states evolves in accordance with a Langevin-type equation in matrix form. The method requires numerical calculation of a matrix square root at each time step, making it a time-consuming algorithm. The same authors also developed a stochastic version of the HH equations that avoids the matrix operations. Although the former version captures the microscopic dynamics efficiently [19], the latter fails to produce accurate enough statistics of spike generation [20,21].

More recently, a model based on stochastic renormalization [22] and alternative diffusion models that need no matrix square root calculation [7,13,23] were introduced. However, these models are not without their own shortcomings. The model of Ref. [22] was developed for a special membrane. The model of Ref. [23] can suffer significant loss in accuracy when the rate functions for the gate opening and closing are noisy [24]. The model of Ref. [13] contains some constant parameters the values of which are estimated phenomenologically. The model of Ref. [7] accommodates relatively large numbers of noise terms and differential equations. For a recent comparative study of these models, see Ref. [25]. On the issue of computation time, the study shows that the Güler model [13] is, as expected, the fastest: three times as fast as the Orio and Soudry model [7] and the Linaro model [23]. This result can be easily understood by comparing the structures of these models. Table I shows the numbers of first-order differential equations and noise terms needed in each model for modeling both potassium and sodium channels. It is seen that the Orio and Soudry model accommodates nearly twice the number of first-order differential equations and nearly three times the number of noise terms with respect to the corresponding numbers in the Güler model. Likewise, with respect to the Linaro model. The present model contains the same number of differential equations as the Güler [13] model and one less noise term (see below), and, therefore, it is much faster than the Orio and Soudry model and the Linaro model; more importantly, it provides a simpler self-contained analytic formulation.

TABLE I. Structure of the membrane models.

Model	No_diff_eqs	No_noise_terms
Orio-Soudry [7]	13	14
Linaro *etal.* [23]	14	11
Güler [13]	7	5
Present model	7	4

Using the state transition diagrams given in Figs. 3 and 4, it is straightforward to apply our present formulation to clusters of potassium and sodium channels. In this case, there is a simplicity that we do not need to use the master equation to specify $\langle\psi_r\rangle$ and $\langle\psi_s\rangle$ for neither channel type. Instead, the averages of the gating variables—$\bar{n}$, $\bar{m}$, and $\bar{h}$—can be employed. The averages evolve in accordance with

$$\dot{\bar{n}} = -\beta_n\bar{n} + \alpha_n(1-\bar{n}), \tag{34a}$$

$$\dot{\bar{m}} = -\beta_m\bar{m} + \alpha_m(1-\bar{m}), \tag{34b}$$

$$\dot{\bar{h}} = -\beta_h\bar{h} + \alpha_h(1-\bar{h}), \tag{34c}$$

where α_n and β_n are opening and closing rates of n gates; similarly, α_m and β_m are the rates of m gates and α_h and β_h are the rates of h gates. Then we have for the potassium channels

$$\langle\psi_4\rangle = \bar{n}^4, \tag{35a}$$

$$\langle\psi_3\rangle = 4\bar{n}^3(1-\bar{n}), \tag{35b}$$

and for the sodium channels

$$\langle\psi_{31}\rangle = \bar{m}^3\bar{h}, \tag{36a}$$

$$\langle\psi_{21}\rangle = 3\bar{m}^2(1-\bar{m})\bar{h}, \tag{36b}$$

$$\langle\psi_{30}\rangle = \bar{m}^3(1-\bar{h}). \tag{36c}$$

Here $\langle\psi_4\rangle$ and $\langle\psi_{31}\rangle$ are the average chain densities for the potassium and the sodium channels' relevant states, respectively. We do not need the expectation values corresponding to the other states as these states are not directly connected to the potassium relevant state n_4, or to the sodium relevant state m_3h_1. Note that here $\langle\psi_j\rangle$ $(j = 0,1,2,3,4)$ represents the probability of a potassium channel to have j open n gates and $\langle\psi_{ij}\rangle$ $(i = 0,1,2,3;\ j = 0,1)$ represents the probability of a sodium channel to have i open m gates and j open h gates.

Then, in using our formulation for the potassium channel clusters, one needs to set that

$$\alpha = \alpha_n,\ \ \beta = 4\beta_n,\ \ \langle\psi_s\rangle = \langle\psi_3\rangle,$$

and employ Eqs. (34a) and (35). Subsequently, the density of open potassium channels ψ_4 follows from $\psi_4 = \langle\psi_4\rangle + \phi_r$. For the sodium channel clusters, before the use of the formulation, one has to evaluate Eqs. (28)–(30) with the settings

$$\beta = 3\beta_m + \beta_h,\ \ \alpha_j = \alpha_m,\ \ \alpha_k = \alpha_h,$$

$$\langle\psi_j\rangle = \langle\psi_{21}\rangle,\ \ \langle\psi_k\rangle = \langle\psi_{30}\rangle.$$

The density of open sodium channels ψ_{31} then easily follows. Here $\langle\psi_{31}\rangle$, $\langle\psi_{21}\rangle$, and $\langle\psi_{30}\rangle$ are decided from Eqs. (34b), (34c), and (36). In this use of the formulation, the parameter N corresponds to the number of potassium or sodium channels in the cluster, depending on the channel type under consideration.

In Fig. 5, we make a numerical study of ψ_4 and ψ_{31} using various constant sets of rate values, more specifically, of their means ($\langle\psi_4\rangle$ and $\langle\psi_{31}\rangle$), standard deviations (σ_4 and σ_{31}), and autocorrelation times (τ_4 and τ_{31}). Related results computed using our model are compared with the corresponding microscopic simulation results. It is seen that our model predicts $\langle\psi_4\rangle$, $\langle\psi_{31}\rangle$, σ_4, and σ_{31} with excellent

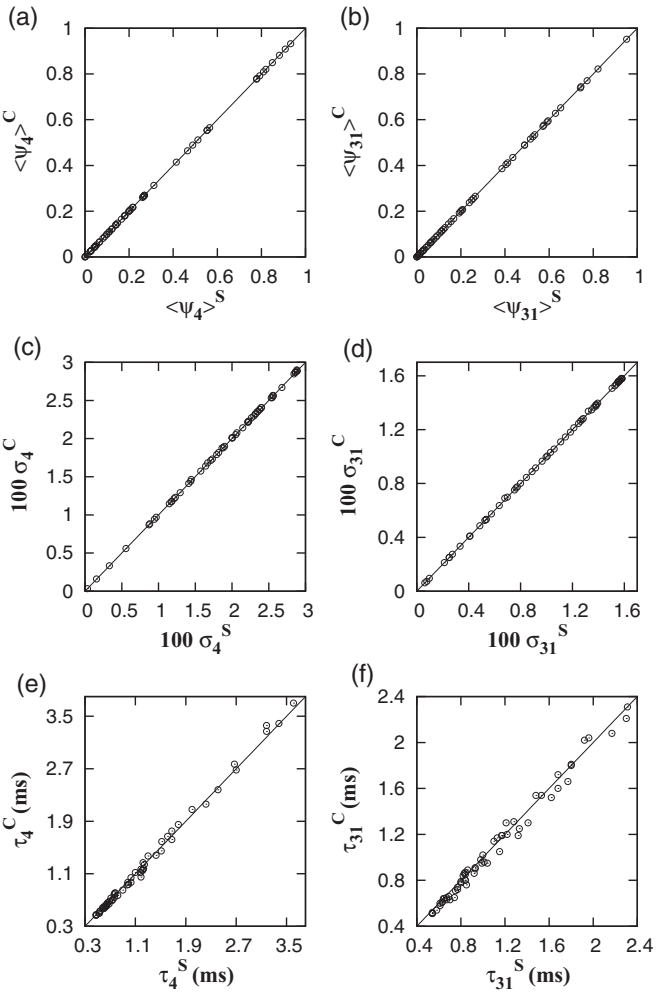

FIG. 5. Numerical experiments performed to examine our model's efficacy for the clusters of 300 potassium channels and 1000 sodium channels. A set of 60 randomly generated rate values in the space of $\{\alpha_n \in (0:1); \beta_n \in (0:0.5)\}$ was used in the potassium experiments; similarly, a set of 60 rate values in the space of $\{\alpha_m \in (0:1); \beta_m \in (0:0.5); \alpha_h \in (0:1); \beta_h \in (0:0.5)\}$ was used in the sodium experiments. Via these rate tuples, various statistical observables were computed from our model (indicated by superscript **C**) and compared with the corresponding microscopic simulation measurements (indicated by superscript **S**). Here σ and τ denote standard deviation and autocorrelation time, respectively. The straight line, put for guidance in each plot, indicates the situation of perfect match between the model and the microscopic simulation. A 400-s time window was used in computing the expectation values.

accuracy. In predicting the autocorrelation times it is not so perfect, but still highly accurate.

Another numerical experiment we perform is on the spiking frequencies in a HH type membrane. Evolution of the transmembrane voltage V in time is decided through the differential equation

$$C\dot{V} = -g_K\psi_4(V - E_K) - g_{Na}\psi_{31}(V - E_{Na}) - g_L(V - E_L) + I,$$

where I is the input current. The values of the constant membrane parameters are as follows: membrane capacitance $C = 1\ \mu\text{F/cm}^2$; maximal potassium conductance $g_K = 36\ \text{mS/cm}^2$; potassium reversal potential $E_K = -12\ \text{mV}$; maximal sodium conductance $g_{Na} = 120\ \text{mS/cm}^2$; sodium reversal potential $E_{Na} = 115\ \text{mV}$; leakage conductance $g_L = 0.3\ \text{mS/cm}^2$; leakage reversal potential $E_L = 10.6\ \text{mV}$; density of potassium channels $= 18\ \text{chns}/\mu\text{m}^2$; density of sodium channels $= 60\ \text{chns}/\mu\text{m}^2$. The rate functions of the membrane are voltage dependent, as given by

$$\alpha_n = (0.1 - 0.01V)/[\exp(1 - 0.1V) - 1],$$
$$\beta_n = 0.125\exp(-V/80),$$
$$\alpha_m = (2.5 - 0.1V)/[\exp(2.5 - 0.1V) - 1],$$
$$\beta_m = 4\exp(-V/18),$$
$$\alpha_h = 0.07\exp(-V/20),$$
$$\beta_h = 1/[\exp(3 - 0.1V) + 1].$$

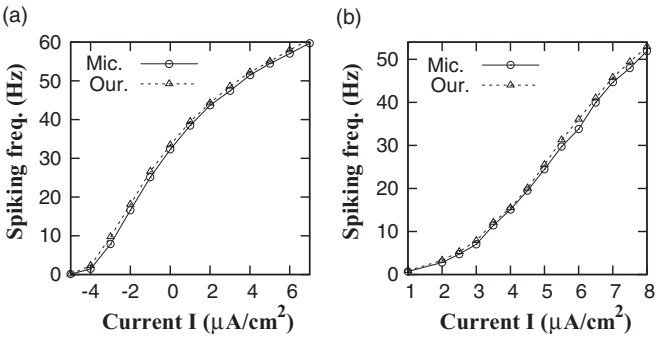

FIG. 6. Mean spiking rates against the input current, displayed by a membrane patch comprised of (a) 360 potassium channels and 1 200 sodium channels (b) 7 200 potassium channels and 24 000 sodium channels. The two plots shown in each figure correspond to result from the microscopic simulations and computation from our model. The averages were computed over a 50-s time window.

Spiking frequencies against the input current are shown in Fig. 6 for two different membrane sizes. It is seen that the frequencies computed from our model are in very good agreement with the frequencies obtained from the microscopic simulations. Recall that in developing our diffusion model we have assumed the transition rates to be constant. However, here the rates are voltage-dependent parameters, and, therefore, they change rapidly during the action of spiking. Nevertheless, it is the subthreshold activity that matters for the initiation of an action potential, and since the voltage does not vary much within that phase of activity, the model still applies. It was shown in Ref. [21] that a nontransient correlation takes place between the fluctuations in the number of open channels and the fluctuations of the transmembrane voltage within the phase of subthreshold activity. This phenomenon (referred to as NCCP) turns out to be the major cause of the elevated excitability and spontaneous firing in limited-size neuronal membranes. A property, crucial for the occurrence of NCCP, is that the autocorrelation time of the fluctuations in the number of open channels is finite but not zero. The accuracy that our present model yields for the spiking frequencies in Fig. 6 is another indication of its precision in capturing fluctuation amplitudes and the autocorrelation times.

VI. CONCLUSION

In this paper, we have studied the temporal evolution of collective fluctuations in Markov chain ensembles. We have in this context formulated a new diffusion approximation to deduce the dynamics of the number of chains in a given relevant state. We have set a theoretical argument to derive the form of the formulation and put forward a set of criteria, as to be necessarily captured by any consistent approximation scheme, to determine the parameter values and noise variances in it. The formulation is basically in the form of two diffusively coupled Langevin-type equations. The advantage of our formulation lies in its minimal complexity. It always accommodates only two stochastic variables (correspondingly two noise terms) irrespective of the state space size or the transition matrix density, and is not hindered by the matrix square root operations. This was facilitated by treating the effect of the state density fluctuations, other than of the relevant state, collectively rather than using the density fluctuations of the individual states explicitly. We have examined our model's efficacy and accuracy for the clusters of potassium and sodium channels and for the excitability of finite-size membranes. The model was found to yield very good accuracy.

We are currently working on an analytic evaluation of the probability function for the relevant state density and on the extension of the formulation to the case of having an arbitrary number of relevant states. Finally, we remark that the formalism developed here is potentially applicable in diverse fields varying from physics, chemistry, and biology to engineering and economics.

[1] J. R. Norris, *Markov Chains* (Cambridge University Press, Cambridge, UK, 1998).

[2] N. G. Van Kampen, *Stochastic Processes in Physics and Chemistry*, 3rd ed. (North-Holland, Amsterdam, 2007).

[3] T. G. Kurtz, Stochastic Proc. Their Appl. **6**, 223 (1978).

[4] P. H. Baxendale and P. E. Greenwood, J. Math. Biol. **63**, 433 (2011).

[5] R. F. Fox and Y. N. Lu, Phys. Rev. E **49**, 3421 (1994).

[6] P. K. Pollett and A. Vassallo, Adv. Appl. Probab. **24**, 875 (1992); D. T. Gillespie, J. Chem. Phys. **113**, 297 (2000); I. Nåsell, Math. Biosci. **179**, 1 (2002); D. Clancy, J. Appl. Probab. **42**, 726 (2005); A. D. Barbour and A. Pugliese, Ann. Appl. Probab. **15**, 1306 (2005); J. V. Ross, J. Math. Biol. **52**, 788 (2006); R. J. Gibbens, P. J. Hunt, and F. P. Kelly, in *Disorder in Physical Systems*, edited by G. R. Grimmett and D. J. A. Welsh (Oxford University Press, Oxford, UK, 1998), pp. 113–127; A. J. McKane and T. J. Newman, Phys. Rev. Lett. **94**, 218102 (2005).

[7] P. Orio and D. Soudry, PLoS One **7**, e36670 (2012).

[8] B. Mélykúti, K. Burrage, and K. C. Zygalakis, J. Chem. Phys. **132**, 164109 (2010).

[9] C. E. Dangerfield, D. Kay, and K. Burrage, Phys. Rev. E **85**, 051907 (2012).

[10] E. J. Allen, L. J. S. Allen, A. Arciniega, and P. E. Greenwood, Stochastic Anal. Appl. **26**, 274 (2008).

[11] B. Hille, *Ionic Channels of Excitable Membranes*, 3rd ed. (Sinauer Associates, Sunderland, MA, 2001).

[12] M. C. Wang and G. E. Uhlenbeck, Rev. Mod. Phys. **17**, 323 (1945).

[13] M. Güler, Neural Comput. **25**, 46 (2013).

[14] N. T. Schmandt and R. F. Galàn, Phys. Rev. Lett. **109**, 118101 (2012).

[15] B. Sakmann and N. Neher, *Single-Channel Recording*, 2nd ed. (Plenum, New York, 1995).

[16] A. L. Hodgkin and A. F. Huxley, J. Physiol. **117**, 500 (1952).

[17] R. Fitzhugh, J. Cell. Comp. Physiol. **66**, 111 (1965); E. Skaugen and L. Walloe, Acta Physiol. Scand. **107**, 343 (1979).

[18] C. C. Chow and J. A. White, Biophys. J. **71**, 3013 (1996).

[19] J. H. Goldwyn, N. S. Imennov, M. Famulare, and E. Shea-Brown, Phys. Rev. E **83**, 041908 (2011).

[20] H. Mino, J. T. Rubinstein, and J. A. White, Ann. Biomed. Eng. **30**, 578 (2002); S. Zeng and P. Jung, Phys. Rev. E **70**, 011903 (2004); I. C. Bruce, Ann. Biomed. Eng. **37**, 824 (2009); B. Sengupta, S. B. Laughlin, and J. E. Niven, Phys. Rev. E **81**, 011918 (2010).

[21] M. Güler, J. Comput. Neurosci. **31**, 713 (2011).

[22] M. Güler, Phys. Rev. E **76**, 041918 (2007).

[23] D. Linaro, M. Storace, and M. Giugliano, PLoS Comput. Biol. **7**, e1001102 (2011).

[24] M. Güler, Neural Comput. **25**, 2355 (2013).

[25] P. F. Rowat and P. E. Greenwood, Front. Comput. Neurosci. **8**, 111 (2014).